Research Paper

Investigation of hERG1b Influence on hERG Channel Pharmacology at Physiological Temperature

Aziza El Harchi[1], Dario Melgari[1], Henggui Zhang[2], Jules C. Hancox[1,2]

[1]School of Physiology, Pharmacology and Neuroscience, Biomedical Sciences Building, The University of Bristol, Bristol, BS8 1TD, [2]Biological Physics Group, School of Physics and Astronomy, The University of Manchester, Manchester, M13 9PL, UK

Abstract

Objective: To compare the inhibitory potencies of selected drugs (chloroquine, fluoxetine, cisapride, and ebastine [EBA]) on human Ether-a-go-go-Related Gene (hERG) potassium channel current carried by either hERG1a or co-expressed hERG 1a/1b channel isoforms. **Materials and Methods:** Measurements of hERG current (I_{hERG}) were made at 37°C from HEK-293 cells expressing either the hERG1a isoform or co-expressing hERG1a and 1b isoforms. A standard "square" waveform voltage protocol was used to elicit I_{hERG}, and tail current measurements were used to construct concentration-response relations for each drug. **Results:** For fluoxetine, cisapride, and chloroquine, the observed potencies of inhibition of I_{hERG} were similar between hERG1 and 1a/1b expression conditions. Further experiments in which the hERG1b isoform was expressed alone also failed to show different potencies from hERG1a for these drugs. Fluoxetine was also tested at room temperature and showed similar potencies against hERG 1a and 1a/1b. EBA was more potent against hERG1a than hERG1a/1b with respective half maximal inhibitory concentration (IC_{50}) values of 32 nM (95% confidence interval [CI] 24 nM–43 nM) and 185 nM (CI 114 nM–304 nM), a 5.8-fold difference. At ambient temperature, EBA was also more potent against hERG1a than 1a/1b, with a 2.4-fold difference in IC_{50}. **Conclusion:** Comparison of these findings with prior planar patch-clamp data suggests that automated patch-clamp data on hERG1a/1b versus hERG 1a at ambient temperature cannot automatically be extrapolated to manual patch clamp at 37°C. The results with EBA highlight that, during hERG screening of novel drugs, there is a case for promising candidates to incorporate some measurements on hERG1a/1b as well as hERG1a channels.

Keywords: Arrhythmia, chloroquine, cisapride, ebastine, fluoxetine, hERG pharmacology, hERG1a/1b, hERG1b, potassium channel, QT interval

Introduction

In the human heart, the rapid delayed rectifier K^+ current (I_{Kr}) contributes significantly to ventricular action potential (AP) repolarization and to set the duration of the QT interval of the electrocardiogram.[1-4] The pore-forming (α) subunit of the I_{Kr} channel is encoded by human Ether-à-go-go-Related Gene (*hERG*) and functional channels are comprised of hERG subunit tetramers.[5] Several (h)ERG1 isoforms have now been identified; of these, only (h)ERG1a and (h)ERG1b seem likely to comprise functional sarcolemmal I_{Kr} channel proteins.[6-11] hERG 1a and 1b are alternate transcripts of *hERG,* with the hERG1b isoform possessing a shorter, distinct N terminus, which lacks the first 16 amino acid residues that in 1a interact with the S4-S5 linker and modulate open-state stability during channel gating.[6-7,12-14] Consequently, ionic current (I_{hERG}) carried by channels incorporating the hERG1b isoform ($I_{hERG1a/1b}$) exhibits markedly faster deactivation than those containing hERG1a alone (I_{hERG1a}).[9-15] In addition, I_{hERG} carried by (h)ERG1a/1b channels has been reported to show faster activation and faster recovery from inactivation than (h) ERG1a expressed alone.[9]

Biochemical evidence for a role for hERG1b in native I_{Kr}, includes co-immunoprecipitation of ventricular (h)ERG1b protein with (h) ERG1a and their co-localization to the T-tubules in ventricular myocytes.[8] In cardiomyocytes derived from human-induced pluripotent stem cells (iPSCs), knockdown

Access this article online	
Quick Response Code:	Website: www.jpharmacol.com
	DOI: 10.4103/jpp.JPP_158_17

Address for correspondence: Jules C. Hancox, School of Physiology, Pharmacology and Neuroscience, Biomedical Sciences Building, The University of Bristol, Bristol, BS8 1TD, UK. E-mail: jules.hancox@bristol.ac.uk

How to cite this article: El Harchi A, Melgari D, Zhang H, Hancox JC. Investigation of hERG1b influence on hERG channel pharmacology at physiological temperature. J Pharmacol Pharmacother 2018;9:92-103.

Received: 10-12-2017 **Revised:** 25-02-2018 **Accepted:** 05-06-2018

of hERG1b using shRNA has been shown to decrease I_{Kr} markedly.[16] Genetic screening of the (h)ERG1b-specific exon in 269 unrelated long QT syndrome (LQTS) patients with no identified mutations in the usual LQTS candidate genes uncovered a patient with a (h)ERG1b exon-specific N-terminal mutation (A8V);[9] this greatly reduced both (h) ERG1b protein levels and (h) ERG1a/1b whole-cell conductance.[9] A second hERG1b-specific mutation (R25W) has recently been identified in a case of intrauterine fetal death.[17] These findings strongly implicate hERG1b as a component of human cardiac I_{Kr} channels. In recombinant systems, hERG1a and 1b form functional heteromers rather than co-existing as pools of distinct homomeric channels.[6-8,15,18] The hERG1b N terminus contains an "RXR" endoplasmic reticulum (ER) retention signal that limits the surface expression of homomeric hERG1b channels.[18] hERG1a helps overcome this retention signal and promote hERG1b trafficking to the cell surface,[18] with hERG1a/b N terminal interactions occurring within the ER to enable hetero-oligomerization.[15]

The I_{Kr}/hERG channel is a major pharmacological target for antiarrhythmic (Class Ia and III) drugs and also structurally and therapeutically diverse noncardiac drugs linked to the acquired (drug-induced) form of the LQTS (aLQTS) and the related arrhythmia torsades de pointes (TdP).[19-21] The pharmacological promiscuity of hERG appears in part to be attributable to the presence of aromatic amino acids in the S6 helices, which facilitate drug interactions.[22-24] Recent cryo-EM data suggest that hERG possesses deep hydrophobic pockets that surround the central cavity and that may contribute to the channel's sensitivity to diverse drugs.[25] Due to the strong link between I_{Kr}/hERG channel block, aLQTS, and TdP, all new pharmaceuticals undergo screening against I_{Kr}/I_{hERG}, most commonly using automated patch-clamp recording from hERG-expressing mammalian cell lines.[21] Virtually all pharmacological studies have focused on the hERG1a isoform, but questions arise as to whether such investigations should include experiments on channels incorporating hERG1b. Some studies have suggested that (h)ERG1a/1b heteromeric channels may exhibit a shift in sensitivity for some hERG inhibitors.[9,26] Thus, in one study using manual patch-clamp at ambient (room) temperature, the selective I_{Kr}/I_{hERG} inhibitor E-4031 was suggested to exhibit reduced potency for (h) ERG1a/1b channels compared to hERG 1a alone, a difference associated with a differential time course of inhibition.[9] However, a recent independent study, also conducted using manual patch-clamp at ambient temperature, has reported no significant difference between hERG1a and hERG1b in the effects of 50 and 100 nM E-4031.[27] On the other hand, a study using automated (planar) patch clamp experiments at ambient temperature has reported differences between hERG1a and hERG1a/1b in blocking potency for a number of drugs.[26] Manual patch-clamp remains the "gold standard" method for the assessment of hERG channel pharmacology,[21] and the present study was undertaken to address the lack of comparative pharmacological data for hERG1a and 1a/1b at mammalian physiological temperature.

Materials and Methods

Maintenance of cells and cell transfection

All recordings were made from HEK-293 cells either stably expressing hERG1a alone (provided by Professor Craig January) or transiently transfected with hERG1b alone or together with hERG1a. The hERG1b plasmid construct was provided by Professor Gail Robertson. Cells were passaged using a nonenzymatic agent (Enzyme Free, Chemicon International) and maintained as previously described.[28] Experiments on hERG 1a employed the stable cell line. For experiments on homomeric 1b channels, 24 h after plating cells out, they were transiently transfected with 0.5 µg of the hERG 1b construct using Lipofectamine™ LTX (Invitrogen, Fisher Scientific, Loughborough, UK) according to the manufacturer's instructions. For experiments on co-expressed hERG1a/1b, 0.25 µg of each of the hERG 1a and 1b constructs were co-transfected.[28] Expression plasmid encoding CD8 was also added (in pIRES, donated by Dr. I Baró and Dr. J Barhanin) as a successful marker of transfection. Cells were plated onto small sterilized collagen-coated glass coverslips 6 h after transfection and recordings were made after at least 24 h incubation at 37°C. Successfully transfected cells (positive to CD8) were identified using Dynabeads® (Invitrogen).

Electrophysiological recordings

For whole-cell patch-clamp recording, cells were continuously superfused at physiological temperature (37°C) or at room temperature (22°C–24°C) with an external solution containing (in mM): 140 NaCl, 4 KCl, 2.5 $CaCl_2$, 1 $MgCl_2$, 10 glucose, and 5 HEPES (titrated to pH 7.45 with NaOH). Patch-pipettes (Corning 7052 glass, AM Systems, Sequim, US) were pulled and heat polished (Narishige MF83, Narishige Tokyo, Japan) to 2.5–4 MΩ. The pipette dialysate contained (in mM): 130 KCl, 1 $MgCl_2$, 5 EGTA, 5 MgATP, and 10 HEPES (titrated to pH 7.2 using KOH). Recordings of hERG current (I_{hERG}) were made using an Axopatch 200 amplifier (Axon Instruments, Molecular devices, Sunnyvale, CA, USA) and a CV201 head stage. Between 70% and 80% of pipette series resistance was compensated. Voltage-clamp commands were generated using "WinWCP" (John Dempster, Strathclyde University).

Drug selection and preparation

Fluoxetine is a selective serotonin reuptake inhibitor that has been associated with cases of tachycardia and syncope through inhibition of the hERG channel.[29] It was selected for this study because in planar patch-clamp experiments at ambient temperature, fluoxetine has been reported to be more potent against hERG 1a/1b than against 1a.[26] Ebastine (EBA) is a second-generation H1 receptor antagonist that produces modest prolongation of the QT_c interval at high concentrations (5–10 fold clinical doses).[30] It was selected for this study because, like fluoxetine, EBA has been reported *in vitro* to be more potent against hERG 1a/1b than against 1a.[26] Chloroquine is an antimalarial agent that like fluoxetine exhibits a fast open hERG channel block[31] and can prolong the QT interval.[32,33] Cisapride is a gastric prokinetic drug that exhibits high-affinity gated-state-dependent block of the hERG channel,[34,35] produces QT interval prolongation, and was withdrawn from clinical use due to cases of severe cardiac arrhythmias.[36,37]

Chloroquine-diphosphate and fluoxetine hydrochloride (Sigma, Paisley, UK) were dissolved in deionized water (Milli-Q, Millipore Limited, Watford, UK) to produce stock solutions of, respectively, 50 mM and 10 mM. Both cisapride monohydrate and EBA (Sigma, UK) were dissolved in DMSO (Sigma, UK) at a stock concentration of 10 mM. All stock solutions were diluted to produce stock solutions ranging down to 1 mM and at least to 1:1000 fold with Tyrode's solution to achieve concentrations stated in the Results section. External solutions were applied using a home-built, warmed, and rapid solution exchange device.

Concentration-response relations shown in the "Results" section were not obtained as cumulative concentration-response relations and, typically, one drug concentration was tested per cell recording.

Electrophysiology data analysis

I_{hERG} tail amplitude was measured between the peak of the outward I_{hERG} tail and the current elicited by the brief prepulse to − 40 mV, in the absence of significant I_{hERG} activation.[28,38,39]

Fractional block of the I_{HERG} tail was determined using the following equation:

Fractional block = $1 - (I_{hERG-drug}/I_{hERG-control})$ (Equation 1)

where $I_{hERG\text{-}drug}$ and $I_{hERG\text{-}control}$ represent "tail" current amplitudes in control and drug containing solutions, respectively.

Concentration-response relations were fitted using the following equation:

Fractional block = $1/(1+ (IC_{50}/[DRUG])^{n_H})$ (Equation 2)

where half maximal inhibitory concentration (IC_{50}) is drug producing half-maximal inhibition of the I_{HERG} tail and n_H is the Hill coefficient for the fit. Drug exposures were kept <10 min at 37°C and correction for current run-down was not performed. Concentration-response relations for the different expression conditions were measured at equivalent periods of drug exposure, allowing "isochronal" concentration-response relations to be constructed.

Mean values in the text are presented either as mean ± standard error of mean or (for IC_{50} and n_H values) as mean ±95% confidence intervals (CIs). Statistical analysis was performed using analysis of variance (ANOVA) or *t*-tests as appropriate (GraphPad Prism v5, Graphpad Software Inc, LaJolla, USA). P <0.05 was considered statistically significant.

Results

Concentration-dependent inhibition of hERG1a and hERG1a/1b by ebastine at 37°C and 24°C

The sensitivity of I_{hERG} to drugs was determined by repetitive application (every 12 s) of a "standard" voltage protocol that has been used in numerous prior I_{hERG} pharmacology studies from our laboratory.[28,38-41] The protocol comprised of a 2-s depolarizing voltage command from a holding potential of −80 mV to + 20 mV followed by a 4-s repolarizing step to −40 mV. Each application of the protocol was preceded by a brief (50 ms) prepulse from − 80 to − 40 mV to monitor instantaneous leak current and thus facilitate accurate I_{hERG} tail measurement (see Methods section). Figure 1 shows typical examples of I_{hERG1a} [Figure 1Ai] and $I_{hERG1a/1b}$ [Figure 1Aii] elicited by repetitive applications of the voltage protocol shown in the lower panels of Figure 1Ai and Aii in the absence and presence of EBA. Currents were recorded in control and after 8 min of drug superfusion, at quasi-steady-state block [0.1 µM EBA in Figure 1A]. For each concentration, the mean fractional block of outward I_{hERG} tail at −40 mV was calculated using equation 1 and plotted as shown in Figure 1B and fitted with equation 2 to obtain concentration-response relations. The fit to the concentration-response plot for inhibition of I_{hERG1a} yielded an IC_{50} of 32 nM (CI 24 nM–43 nM) and an n_H of 0.79 (CI 0.66–0.93). For hERG1a/1b, it was 185 nM (CI 114 nM–304 nM) (P < 0.01) (n_H) of 0.67 (CI 0.35–0.97). Thus, the IC_{50} for hERG1a/1b was ~5.8 fold that of hERG 1a alone. To characterize further the consequences of co-expression of hERG1a with hERG1b, we studied the time course of I_{hERG} inhibition and effect of drug block on I_{hERG} time constants of deactivation for the two expression conditions. Tail currents on repolarization to −40 mV were fitted using a bi-exponential to derive the fast τ_1 and slow τ_2 time constants of deactivation in control and after 8-min perfusion of EBA 0.1 µM. As previously reported, time constant values of declining $I_{hERG1a/1b}$ on repolarization to −40 mV showed marked acceleration of hERG1a/1b channel deactivation compared to hERG1a.[41] At 8 min of exposure, 0.1 µM EBA reduced I_{hERG1a} by 75.7% ± 3.8% (n = 8); the time constants of deactivation on repolarization to − 40 mV were accelerated by this drug concentration: τ_1 was 242.4 ± 22.6 ms in control and 187.6 ± 21.3 ms in EBA (n = 8; P < 0.001 vs. control). τ_2 in control was 1527.2 ± 136.2 ms (n = 8) and 860 ± 92.7 ms in EBA (n = 8; P < 0.001 vs. control). During 8 min of comparable recording of I_{hERG1a} in control solution, there was no significant change in deactivation time-course (data not shown). Superfusion of EBA at the same concentration produced 45.2 ± 5.7% block of $I_{hERG1a/1b}$ (n = 5; P < 0.01 vs. 1a) with no significant change to deactivation rate (no significant difference [NSD] vs. control for both time constants). Time courses of inhibition were determined as the fraction of inhibited tail current on repolarization to − 40 mV against the time of drug

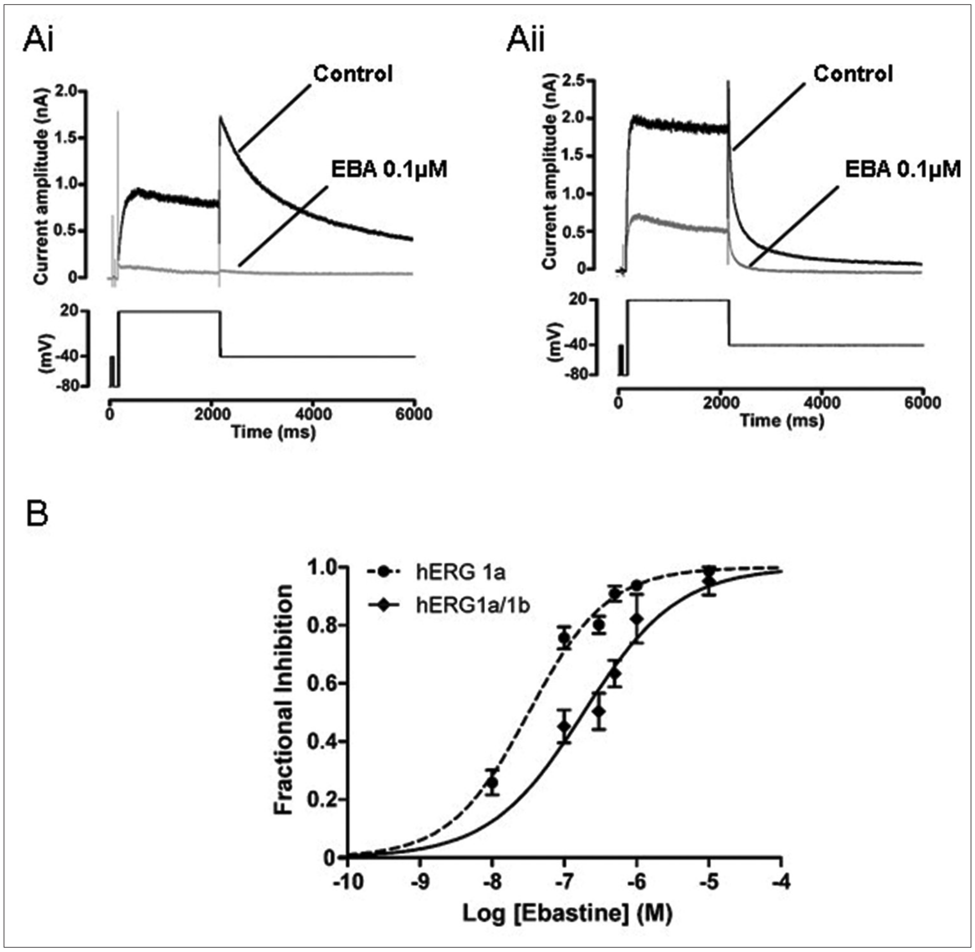

Figure 1: (A) Representative traces for I_{hERG1a} (Ai) and $I_{hERG1a/1b}$ (Aii) before and during exposure to 0.1 μM ebastine at 37°C. Lower panels show voltage protocols used. (B) Isochronal concentration-response relationships at 8 min of drug exposure. hERG 1a (circles; IC_{50} 32 nM [confidence interval 24–43 nM]) and hERG 1a/1b (diamonds; IC_{50} 185 nM [confidence interval 114–304 nM]; $P < 0.05$ vs. 1a) ($n = 4$–6 cells per concentration), with n_H values of 0.79 (confidence interval 0.66–0.93) for hERG1a and of 0.67 (confidence interval 0.35–0.97) for hERG 1a/1b

application (data not shown); a single exponential fit to the averaged plots yielded a time constant τ of 246.5 ± 17.4 s (n = 8 cells) for hERG1a and of 207.9 ± 39.1 s for hERG1a/1b (n = 5 cells; [NSD], $P > 0.05$ vs. 1a).

Co-expression of hERG 1a with hERG1b has previously been associated with a >4-fold leftward shift in IC_{50} compared to hERG 1a in planar patch-clamp experiments at room temperature.[26] To enable comparison with that study, we determined sensitivity to EBA at room temperature of both hERG1a and hERG1a/1b. Figure 2Ai and Aii show typical records for I_{hERG} inhibition by 1 μM EBA for hERG1a [Figure 2Ai] and hERG a/1b [Figure 2Aii] at 24°C. Concentration-response data were obtained at 8 min of drug exposure and are shown in Figure 2B. These yielded an IC_{50} of 820 nM (CI 446–1.5 μM) (n = 4–5 cells per concentration; n_H = 0.72 [CI 0.67–1.11]) for hERG 1a and 1.93 μM (CI 1.23–3.02 μM) (n = 4–5 cells per concentration; $P < 0.05$; n_H = 1.19 [CI 0.65–1.73]) for 1a/1b. Thus, at ambient temperature, co-expression of hERG 1a with 1b resulted in a directionally (rightward) similar shift in IC_{50} to that seen at 37°C, although it was smaller (2.4 fold that for hERG 1a) in magnitude.

Concentration-dependent inhibition of hERG1a and hERG1a/1b by fluoxetine, chloroquine, and cisapride at 37°C

We also compared the effects of fluoxetine on I_{hERG} carried by hERG1a and co-expressed hERG 1a/1b. Figure 3A shows representative traces before application (control) and in the presence of fluoxetine (1 μM) for hERG1a [Figure 3Ai] and hERG1a/1b [Figure 3Aii]. Inhibition of the elicited current typically reached a quasi-steady-state block within 3 min of drug superfusion. Isochronal concentration-response relations for fluoxetine effects on hERG1a and 1a/1b are shown in Figure 3B. For hERG1a, the derived IC_{50} was 1.40 μM (CI 1.20–1.65 μM) and a Hill coefficient n_H of 1.62 (CI 1.17–2.07), which is in good agreement with previously reported data.[29] Co-expression of hERG1a with hERG1b was associated with a negligible shift in I_{hERG} sensitivity to fluoxetine with an IC_{50} value for inhibition of $I_{hERG1a/1b}$ of 1.36 μM (CI 0.99–1.87 μM) ($P > 0.05$ vs. 1a; with an n_H for the fit of 0.93 [CI 0.64–1.22]). We also assessed the effect of fluoxetine on deactivation rate of I_{hERG} carried by hERG1a and hERG1a/1b channels. For I_{hERG1a}, the estimated

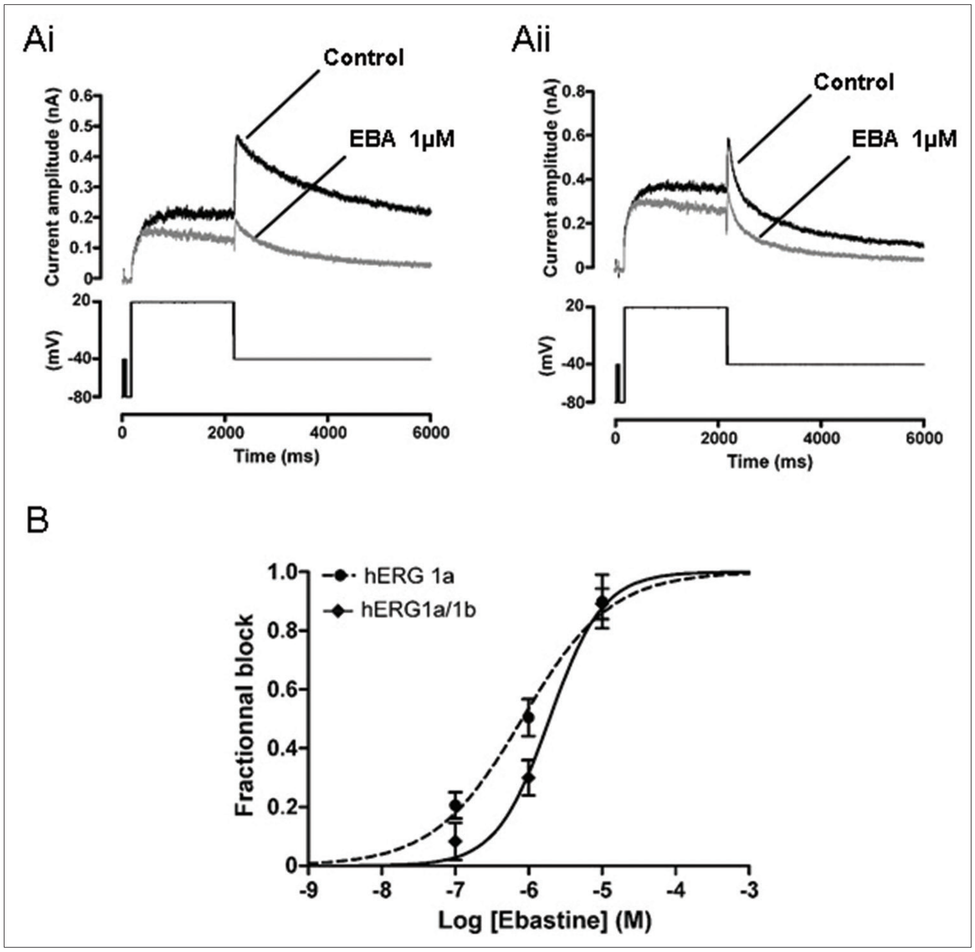

Figure 2: (A) Representative traces for I_{hERG1a} (Ai) and $I_{hERG1a/1b}$ (Aii) before and during exposure to 1 μM ebastine at 24°C. Lower panels show voltage protocols used. (B) Isochronal concentration-response relationships at 8 min of drug exposure. hERG 1a (circles; IC_{50} 820 nM [confidence interval 0.45–1.5 μM]) and hERG 1a/1b (diamonds; IC_{50} 1.93 μM [confidence interval 1.23–3.02 μM]) showed differences in inhibitory potency ($P < 0.05$; $n = 4–5$ cells per concentration) with n_H values of 0.72 (confidence interval 0.67–1.11) for hERG1a and of 1.19 (confidence interval 0.65–1.73) for hERG 1a/1b

fast time constant τ_1 was 176.0 ± 38.2 ms in control versus 227.7 ± 62.4 ms ($n = 6$, $P > 0.05$ vs. control) in drug. Similarly, the slow time constant τ_2 before and after drug application remained unchanged: τ_2 was 1236.5 ± 287.8 ms ($n = 6$) and 1414.3 ± 360.1 ms ($n = 6$ cells; $P > 0.05$ vs. in control) in control and drug, respectively. Fits to deactivating $I_{hERG1a/1b}$ tails yielded a τ_1 of 74.1 ± 9.3 ms ($n = 6$, $P < 0.05$ vs. I_{hERG1a}) and a τ_2 of 832.1 ± 87.8 ms ($n = 6$, $P < 0.05$ vs. I_{hERG1a}). Similar to hERG1a, both time constants remained unchanged after drug application with estimated values for τ_1 and τ_2 of, respectively, 73.9 ± 7.2 ms ($n = 6$; $P > 0.05$ vs. in control) and 776.6 ± 63.2 ms ($n = 6$; $P > 0.05$ vs. in control). The time course of hERG current inhibition by fluoxetine (1 μM) was similar between hERG 1a and 1a/1b, with time constants of inhibition of 78.3 ± 19.9 s ($n = 5$ cells) for hERG1a and 86.1 ± 15.2 s ($n = 6$ cells; NSD, $P > 0.05$ vs. 1a) for hERG1a/1b.

Thus, in recordings at 37°C, fluoxetine inhibited I_{hERG} carried by co-expressed hERG1a/1b with similar potency and time course to that carried by hERG 1a alone. This differs from prior work with planar patch-clamp at ambient temperature, in which fluoxetine was reported to be more potent against hERG 1a/1b than against 1a.[26]

Similar experiments were carried out to assess the potency of chloroquine [Figure 4]. We found chloroquine to inhibit hERG1a and hERG1a/1b at 37°C with isochronal IC_{50} values, respectively, of 0.89 μM (CI 0.63–1.27 μM) ($n = 4–5$ cells per concentration; $n_H = 0.75$ [CI 0.55–0.95]) and 1.43 μM (CI 1.02–2.0 μM) ($P > 0.05$ vs. 1a; $n = 5–7$ cells per concentration; $n_H = 0.81$ [CI 0.58–1.05]). The time constants of I_{hERG} inhibition by 1 μM chloroquine were, respectively, 62.5 ± 21.5 s and 82.0 ± 23.6 s ($n = 5$ and 5; NS, vs. 1a $P > 0.05$). No change to the time constants of deactivation on repolarization to −40 mV was observed.

We also investigated the sensitivity of both channel expression conditions to cisapride [Figure 5]. Cisapride was found to inhibit hERG1a with an IC_{50} of 40.8 nM (CI 26.2–63.7 nM) and an n_H of 0.85 (CI 0.47–1.23) ($n = 5–7$ cells per concentration). 30 nM of cisapride inhibited I_{hERG1a} with a time constant τ of 147.1 ± 29.4 s ($n = 8$ cells) and was not associated with a

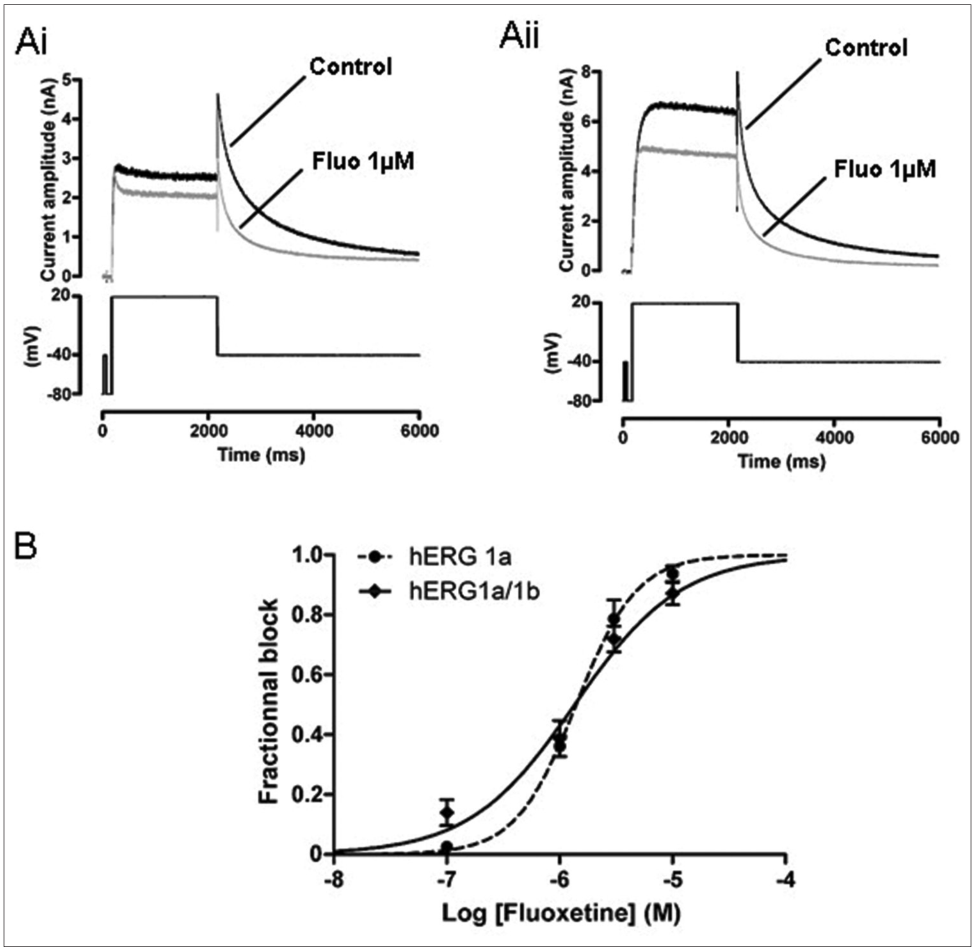

Figure 3: (A) Representative traces for I_{hERG1a} (Ai) and $I_{hERG1a/1b}$ (Aii) before and during exposure to 1 μM fluoxetine at 37°C. Lower panels show voltage protocols used. (B) Isochronal concentration-response relationships at 3 min of drug exposure. hERG 1a (circles; IC_{50} 1.40 μM [confidence interval 1.20–1.65 μM]) and hERG 1a/1b (diamonds; IC_{50} 1.36 μM [confidence interval 0.99–1.87 μM]) showed similar IC_{50} values (n = 4–6 cells per concentration; $P > 0.05$), and an apparently modest but statistically insignificant difference in n_H: n_H = 1.6 (confidence interval 1.17–2.07) for hERG1a and n_H = 0.9 (confidence interval 0.64–1.22) for hERG 1a/1b [$P > 0.05$ for analysis of variance comparison of these values and that for hERG 1b in Figure 6]

change in I_{hERG1a} rate of deactivation ($P > 0.05$ vs. control). hERG 1a/1b channels were inhibited with an IC_{50} of 52.4 nM (CI 33.5–82.0 nM) ($P > 0.05$ vs. 1a, n = 4–10 cells per concentration) and n_H of 0.65 (CI 0.37–0.94). Time course of inhibition of $I_{hERG1a/1b}$ by 30 nM cisapride was similar to that of I_{hERG1a} (τ =119.9 ± 25.4 s; n = 8 cells; NSD, vs. I_{hERG1a} $P > 0.05$). The time course of deactivation of $I_{hERG1a/1b}$ under drug superfusion was similar to that measured before drug exposure (n = 8 cells; $P > 0.05$ vs. control).

Concentration-dependent inhibition of hERG1b by fluoxetine, chloroquine, and cisapride at 37°C

Unlike EBA, fluoxetine, chloroquine, and cisapride showed little difference in I_{hERG} inhibitory potency between hERG1a and hERG1a/1b expression conditions. There is considerable electrophysiological and biochemical evidence that hERG1a and 1b form functional heteromers rather than co-exist in the cell membrane as pools of distinct homomeric channels.[6-9,18,42] Thus, physiologically relevant information on the effect of hERG1b on drug sensitivity is most likely to derive from comparisons of hERG 1a with co-expressed hERG1a/1b [Figures 1-5], rather than from comparisons with homomeric hERG 1b channels. However, we reasoned that any influence of hERG1b on drug potency might be anticipated to be most evident under conditions in which the hERG1b isoform is expressed alone and that such experiments may therefore have utility for studying inhibitory potency of drugs for which differences from hERG 1a were not seen using co-expressed hERG 1a/1b. Consequently, we conducted further experiments with fluoxetine, chloroquine, and cisapride on hERG1b in the absence of co-transfected hERG1a. Figure 6A shows representative traces of I_{hERG1b} before application (control) and after quasi-steady-state of block by 1 μM fluoxetine [Figure 6Ai], 1 μM chloroquine [Figure 6Aii], or 30 nM cisapride [Figure 6Aiii]. Similar to I_{hERG1a} and $I_{hERG1a/1b}$, the time course of I_{hERG1b} deactivation was assessed using bi-exponential curve fitting of the time course of current decline on repolarization to −40 mV. As anticipated for hERG 1b alone, both deactivation time constants were faster than those for I_{hERG1a} and $I_{hERG1a/1b}$.[9-12,43] Fits to plots

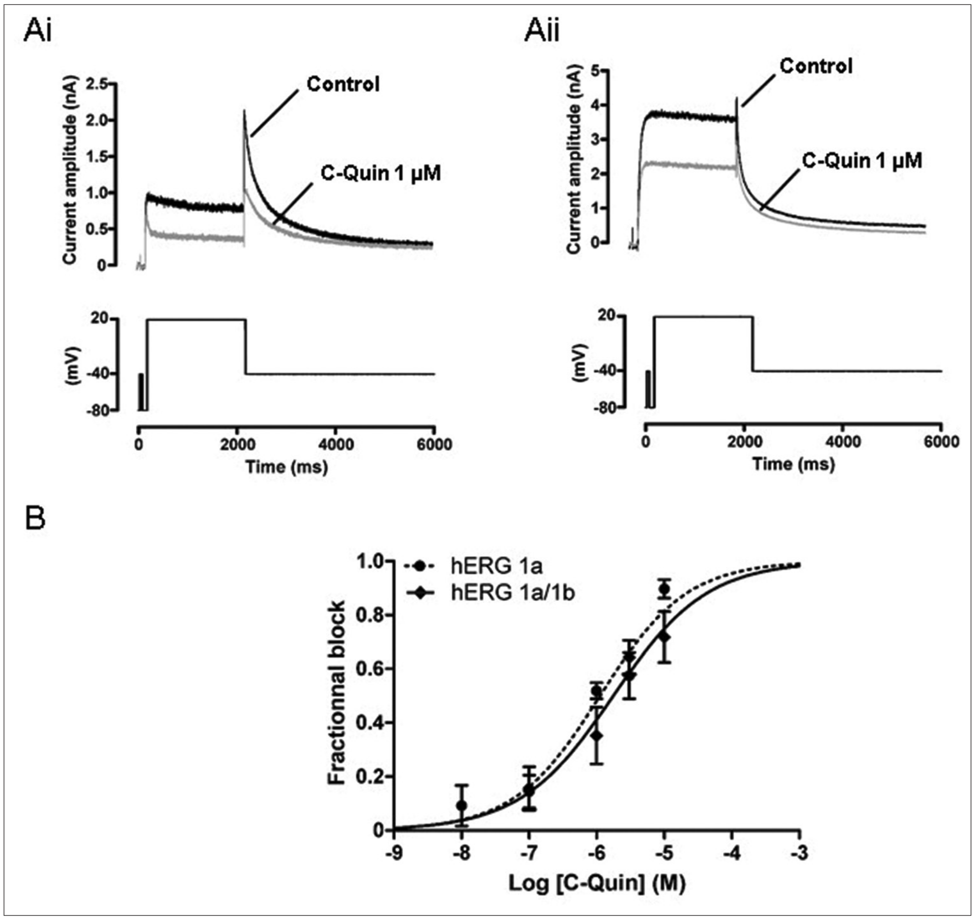

Figure 4: (A) Representative traces for I_{hERG1a} (Ai) and $I_{hERG1a/1b}$ (Aii) before and during exposure to 1 μM chloroquine at 37°C. Lower panels show voltage protocols used. (B) Isochronal concentration-response relationships at 3 min of drug exposure for chloroquine inhibition of hERG1a (circles; IC_{50} 0.89 μM [confidence interval 0.63–1.27 μM]) and hERG1a/1b (diamonds; IC_{50} 1.43 μM [confidence interval 1.02–2 μM]) n = 4–7 cells per concentration (P > 0.05 vs. 1a). Hill coefficients yielded from the fit to dose responses curves were n_H = 0.75 (confidence interval 0.55–0.93) for hERG1a and n_H = 0.81 (confidence interval 0.58–1.05) for hERG 1a1b

of declining current yielded an average τ_1 of 16.8 ± 3.2 ms (n = 6; P < 0.001 vs. 1a) and a τ_2 of 506.9 ± 109.5 ms (n = 6; P < 0.001 vs. 1a). The relative contribution of fast deactivation increased to 93.3 ± 2.2% (n = 6; P < 0.001 vs. 1a) from 44.8 ± 6.0% (n = 6) for 1a and for 65.3 ± 6.0% (n = 6, P < 0.05 vs. 1a) for 1a/1b. Thus, under our conditions, I_{hERG1b} exhibited distinct features that are consistent with the hERG1b isoform's known properties. IC_{50}s for inhibition of I_{hERG1b} were derived from the concentration response curves shown in Figure 6B. Sensitivity to fluoxetine was similar to that of I_{hERG1a} with an estimated IC_{50} for inhibition of I_{hERG1b} of 1.18 μM (CI 0.87–1.60 μM) (n = 4–6 cells per concentration, P > 0.05 vs. 1a; n_H = 1.23 [CI 0.61–1.84]). Chloroquine and cisapride also showed no significant changes in IC_{50} for inhibition of I_{hERG1b}. For chloroquine, the derived IC_{50} was 1.11 μM (CI 0.51–2.41 μM) (n = 4–5 cells per concentration, P > 0.05 vs. 1a; n_H = 0.63 [CI 0.28–0.94]) and 54.5 nM (CI 37.6–79.0 nM) (n = 5–6 cells per concentration, P > 0.05 vs. 1a; n_H = 1.20 [CI 0.46–1.94]) for cisapride. Time constants for inhibition time course were similar to that of I_{hERG1a} for each of the three drugs tested. In addition, both fast and slow time constants of deactivation of I_{hERG1b} on repolarization to −40 mV remained unchanged after drug application.

Concentration-dependent inhibition of hERG1a, hERG1a/1b, and hERG1b by fluoxetine at room temperature

Prior data suggestive of differential pharmacological sensitivity of heteromeric 1a/1b versus homomeric 1a channels were carried out at room temperature.[9,26] Fluoxetine, in particular, was highlighted as a drug that was more potent against hERG1a/1b than 1a in planar patch-clamp at room temperature.[26] We therefore conducted additional experiments on fluoxetine at room temperature. Figure 7Ai-Aiii shows typical traces of currents recorded from cells expressing 1a, co-expressed 1a/1b, or 1b alone in control and after quasi-steady-state of block was reached following perfusion of 3 μM fluoxetine at 24°C. Isochronal concentration-response relations [Figure 7B] for inhibition of 1a, 1a/1b, and 1b I_{hERG} tails yielded IC_{50}s of 1.87 μM (CI 1.48–2.37 μM) (n = 4–6 cells per concentration; n_H = 0.89 [CI 0.67–1.11]) for 1a, 3.02 μM (CI 2.20–4.14 μM) (n = 4–6 cells per concentration;

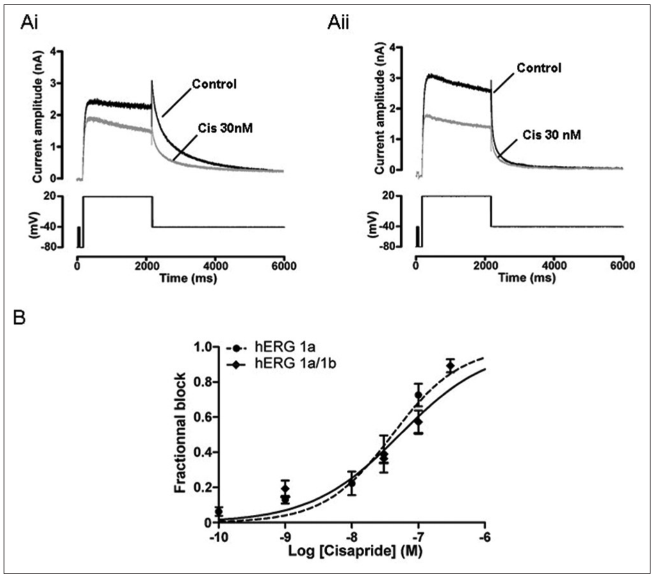

Figure 5: (A) Representative traces for I_{hERG1a} (Ai) and $I_{hERG1a/1b}$ (Aii) before and during exposure to 30 nM cisapride at 37°C. Lower panels show voltage protocols used. (B) Isochronal concentration-response relationships at 5 min drug exposure. hERG 1a (circles; IC_{50} 40.8 nM [confidence interval 26.2–63.7 nM]) and hERG 1a/1b (diamonds; IC_{50} 52.4 nM [confidence interval 33.5–82 nM]) showed similar IC_{50} values (n = 4–10 cells per concentration) (P > 0.05 vs. 1a), with n_H values of 0.85 (confidence interval 0.47–1.23) for hERG1a and of 0.65 (confidence interval 0.37–0.94) for hERG 1a/1b

$P > 0.05$ vs. 1a; $n_H = 1.03$ [CI 0.62–1.44]) for 1a/1b, and 3.31 μM (CI 2.55–4.35 μM) for 1b (n = 4–7 cells per concentration; $P > 0.05$ vs. 1a; $n_H = 0.92$ [CI 0.59–1.24]). Thus, at ambient temperature, co-expression with 1b was associated with a statistically insignificant change in sensitivity to fluoxetine.

Discussion

The need to establish accurate hERG half maximal inhibitory concentration values for drug block

Pharmacological inhibition of I_{Kr}/I_{hERG} is a well-accepted surrogate marker for drug-induced proarrhythmic risk, to the extent that an *in vitro* I_{Kr}/I_{hERG} assay is a mandatory component of current preclinical safety testing of drug candidates under the current ICH S7B guidelines.[21,44,45] However, it is well established that comparatively few individuals who receive particular drugs manifest clinically significant QT_c interval prolongation or TdP arrhythmia and that multiple risk factors determine the overall drug response.[46-48] The precise relationship between I_{hERG} inhibition and TdP is complex and also depends both on whether or not a drug can affect other cardiac ion channels that offset its action on hERG and on the relative potency of the drug against hERG and its intended target(s).[21,44] Through a comprehensive analysis of preclinical and human data, Redfern *et al*. reported that the majority of hERG-interacting drugs without reports of TdP in humans exhibited a >30-fold separation between hERG IC_{50} and effective therapeutic free plasma concentrations,[49] suggesting that a minimal safety margin of 30 fold between C_{max} and hERG IC_{50} may be adequate for compounds in development. It follows that, in the calculation of a drug's safety margin, the precise value of a compound's IC_{50} against I_{hERG}/I_{Kr} assumes some importance. This issue is complicated, however, by the fact that IC_{50} values can differ between expression systems, experimental conditions (particularly temperature), stimulus protocol, and due to interlaboratory variability.[50-55] Virtually, all studies of hERG channel pharmacology have used the hERG 1a isoform, and the growing evidence that native I_{Kr} may involve both hERG 1a and 1b isoforms[6,8,9,15-16] raises a question as to whether or not drug screens for hERG activity should continue to rely on hERG 1a alone or incorporate work on heteromeric hERG 1a/1b channels? This question is particularly timely, as the existing safety testing paradigm is currently under consideration and may be replaced with a highly specified preclinical approach integrating data from a number of different recombinant channels, hiPSC myocytes, and mathematical modeling: The Comprehensive *in vitro* Proarrhythmic Assay (CiPA) paradigm.[56,57]

Comparison between the present study and previous studies

Although manual patch-clamp has the limitation of being low throughput, it remains the gold standard approach for evaluating drug actions on hERG.[21] The present study utilized a standard voltage protocol and temperature to compare the blocking potency of selected drugs against hERG1a and co-expressed hERG1a/1b. An important feature of the use of mammalian cell line recordings at physiological temperature for such experiments is that these conditions minimize differences between properties of recombinant hERG1a channels and native I_{Kr}.[58] Under these conditions, only one of the four drugs examined here showed any statistically significant difference in I_{hERG} IC_{50} between hERG 1a and hERG1a/1b conditions. With our standard protocol, cisapride, chloroquine, and fluoxetine showed no significant difference in potency between hERG1a and hERG1a/1b at physiological temperature. Nor did the hERG 1b isoform alone exhibit altered potency compared to hERG 1a for any of these three drugs. EBA, on the other hand, showed a >5-fold difference between hERG1a and hERG1a/1b IC_{50} at 37°C and >2-fold difference at room temperature. Plasma C_{max} values for EBA after 5 days of daily oral dosing (20 mg) have been reported to reach ~13 nM (5.98 ng/ml).[59] With our IC_{50} values, this would yield safety margin values of between ~2.5 (for hERG 1a) and 14 (for hERG 1a/1b) at physiological temperature. The Kd for EBA against native guinea pig I_{Kr} of 140 nM would give a safety margin of ~11,[60] closer to that seen here for hERG 1a/1b than for hERG 1a alone. A prior study using automated patch-clamp reported differences between hERG1 and hERG 1a/1b in EBA potency, but with μM IC_{50} values (i.e., higher values than seen here for either isoform at physiological temperature or, previously, for native cardiomyocytes[60]). Our isochronal concentration-response relations showed higher IC_{50} values for EBA at room temperature than at 37°C, which may, at least in

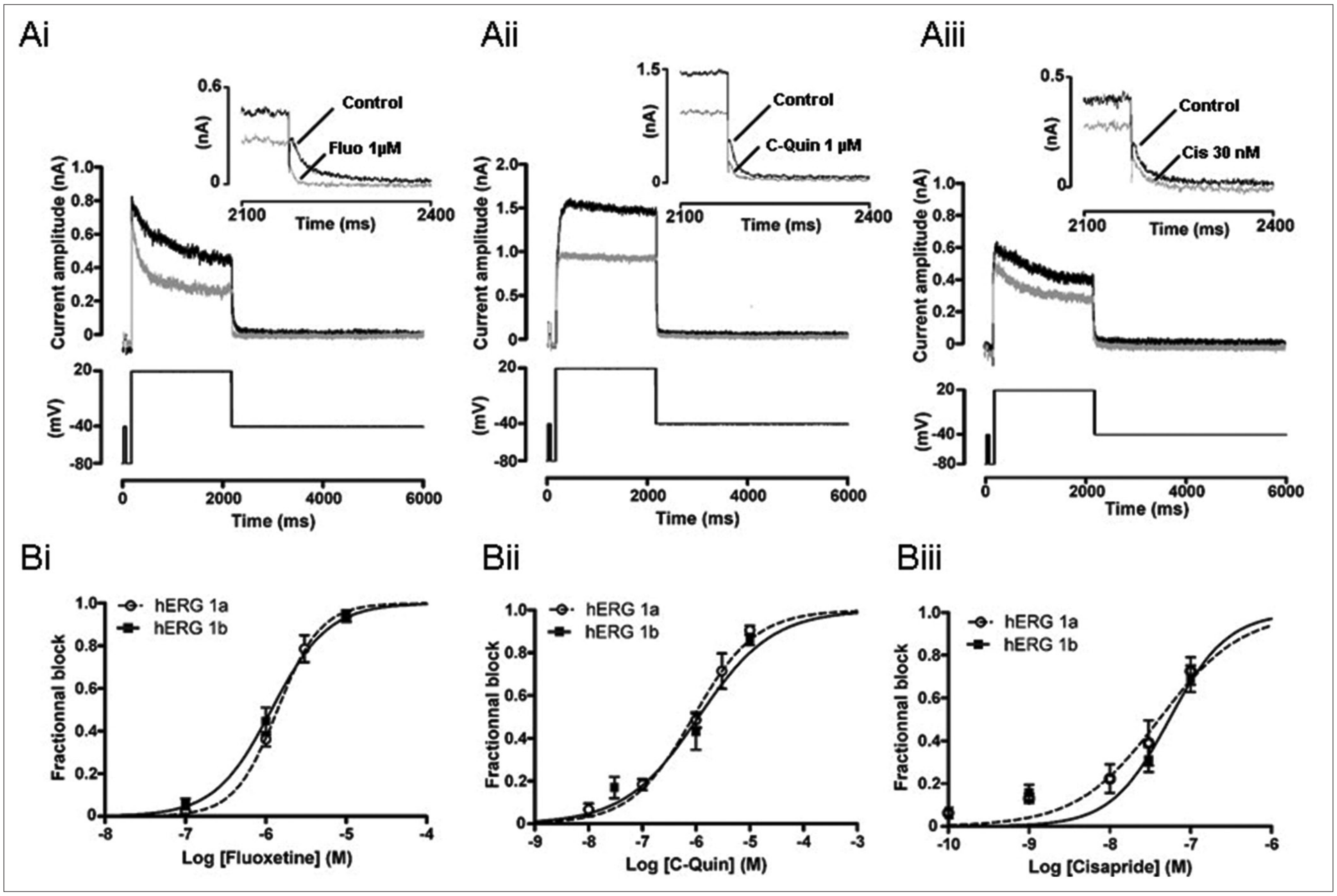

Figure 6: (A) Representative traces for inhibition of I_{hERG1b} by fluoxetine 1 μM (Ai) chloroquine 1 μM (Aii) and cisapride 30 nM (Aiii) at 37°C. Lower panels show voltage protocols used. (B) Isochronal concentration-response relationships. Fluoxetine inhibited I_{hERG1b} with an IC_{50} of 1.18 μM (confidence interval 0.87–1.60 μM) (n_H = 1.23 [confidence interval 0.61–1.84]; *n* = 4–6 cells per concentration), chloroquine with an IC_{50} of 1.11 μM (confidence interval 0.51–2.41 μM) (n_H = 0.63 [confidence interval 0.28–0.94]; *n* = 4–5 cells per concentration) and cisapride with an IC_{50} of 54.5 nM (confidence interval 37.6–79 nM) (n_H = 1.2 [0.46–1.94]; *n* = 5–6 cells per concentration)

part, involve temperature-dependent differences in solubility of the drug[60] and/or reflect more gradual development of block at the lower temperature. Importantly, in contrast to our observations at both physiological and room temperature, the prior published planar patch-clamp data suggested a greater inhibitory potency of EBA against hERG 1a/1b than 1a.[26] The same automated patch-clamp study prior reported fluoxetine to be more potent against hERG 1a/1b than against hERG 1a, which contrasts with our data at both ambient and physiological temperatures. The basis for these differences between studies is not clear, but may be attributable to differences in recording method or voltage protocol.

It should be noted that the fact that we saw no significant deviation from hERG 1a fluoxetine potency even when hERG 1b was expressed alone argues strongly against marked differences in fluoxetine inhibitory potency between hERG 1a and 1b under physiologically relevant conditions.

One prior manual patch-clamp study reported a slower time course of inhibition of hERG1a/1b than hERG 1a by the methanesulphonanilide E-4031 and a 4-fold higher IC_{50} for hERG1a/1b at ambient temperature.[9] Subsequent planar patch-clamp recordings also showed differences between hERG 1a and 1a/1b for E-4031 and the related methanesulphonanilide dofetilide.[26] This class of drugs binds within the hERG channel's inner cavity, interacting strongly with S6 aromatic residues (Y652 and F656) as well as other residues in the S6 and pore-helical regions.[61,62] In structural terms, hERG 1a and 1b differ from one another solely in the N terminal region and so have complete sequence identity over the canonical drug-binding site.[6-7,12] Thus, the same canonical drug-binding site residues within the pore are available in both hERG1a and 1b isoforms. The reported difference between hERG 1a/1b and hERG 1a in E-4031 sensitivity was accounted for by in a kinetic model by inclusion of "N-liganded" states in the hERG1a model that were absent in hERG1a/1b heteromers.[9] This issue is complicated, however, by data from a more recent study employing manual patch-clamp that found similar effects of E-4031 at 50 and 100 nM on hERG1a and 1b isoforms.[27] Of the drugs investigated in the present study, chloroquine and cisapride have been demonstrated to interact strongly with aromatic residues in the canonical drug-binding site.[31,61,63] Mutation of F656 has also been found strongly to impair pharmacological block of I_{hERG} by fluoxetine.[29]

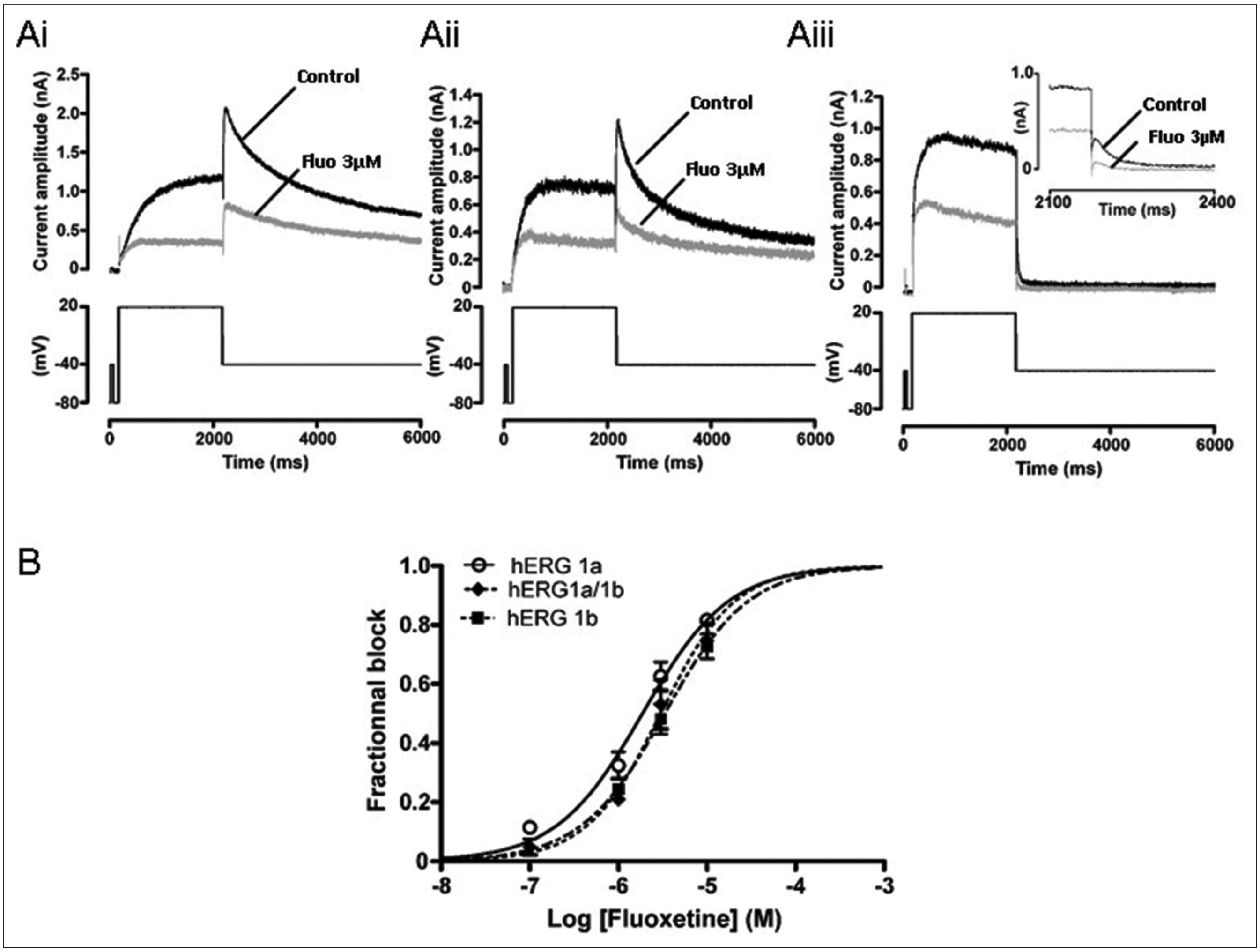

Figure 7: (A) Representative traces for I_{hERG1a} (Ai) $i_{hERG1a/1b}$ (Aii) and I_{hERG1b} (Aiii) before and during exposure to 3 μM fluoxetine at room temperature. Lower panels show voltage protocols used. (B) Concentration-response relationships. At room temperature, fluoxetine inhibited 1a (open circles) with an IC_{50} of 1.87 μM (confidence interval 1.48–2.37 μM). hERG 1a/1b (triangles) and hERG 1b (squares) dose–response relationships showed similar IC_{50} values (n = 4–7 cells per concentration) and were inhibited, respectively, with an IC_{50} of 3.02 μM (confidence interval 2.20–4.14 μM) ($P > 0.05$ vs. 1a) and an IC_{50} of 3.31 μM (confidence interval 2.55–4.35 μM) ($P > 0.05$ vs. 1a)

Thus, binding residues are likely to be similar for these drugs between hERG1a and 1b channel proteins. We have recently reported that the HCN-channel inhibitor ivabradine inhibits hERG1a and 1a/1b with similar IC_{50} values and that drug also interacts with canonical aromatic-binding residues.[28] The process of hERG channel inactivation is important for optimal interactions of a number of drugs with their binding site on the channel.[21,22] In principle, inactivation dependence of inhibition could be influenced for hERG1a/1b by the fact that hERG 1a/1b heteromers have fewer N termini that can interact with the S4-S5 linker and stabilize inactivation.[9,13] By extension, this difference would be anticipated to be greater for homomeric 1b channels. Thus, one might speculate that, at least under our conditions, differences between hERG 1a and 1a/1b or 1b channel kinetics due to the different N termini are insufficient to alter significantly the potency of chloroquine, cisapride, or fluoxetine binding, but are sufficient to reduce EBA binding to the heteromeric channel. To our knowledge, the binding site for EBA on hERG has not yet been mapped, though on the basis of only weak voltage dependence of inhibition of I_{Kr}, it has been suggested that the drug might not interact with the pore region of the channel.[60]

One markedly hERG 1b selective inhibitor, CD-160130, has been identified,[27] inhibiting hERG1b with an approximate 8-fold the potency against hERG 1a.[27] The actions of that drug are resistant to mutation of F656, suggesting that it binds elsewhere from the canonical binding site, though its action does not seem dependent on the hERG1b unique N terminus.[27] CD-160130 has not yet been tested on hERG1a/1b heteromers.[27]

Implications and Conclusions

Three of the four drugs investigated in the present study showed similar inhibitory potency between hERG 1a, hERG1a/1b, and hERG 1b, with a standard hERG screening protocol. Our results with fluoxetine and EBA are notable, as they indicate that data in respect of comparative hERG1a and 1a/1b sensitivities obtained with planar patch-clamp at ambient temperature[26] cannot automatically be extrapolated to manual patch-clamp at 37°C. That said, we do not exclude the possibility that drugs which exhibit little difference in hERG1a and hERG 1a/1b in blocking potency with the protocol deployed in this study might show differences between the two channel isoforms with different voltage stimulation protocols. Indeed, limited additional experiments using a ventricular AP waveform as the voltage command showed no difference between 1a and 1a/1b in inhibition of peak I_{HERG} fluoxetine at a single concentration (1 µM); cisapride however (the action of which on hERG1a has been found to be highly protocol dependent[35]) showed greater block of hERG1a/1b than 1a during the AP waveform at 30 nM (data not shown). Our EBA data indicate that it is possible to obtain significant differences in potency for some drugs between hERG 1a and hERG1a/1b, with the recording conditions employed here. Moreover, our EBA data suggest that, even at a single (ambient) temperature, results may not be readily extrapolated from automated to manual patch-clamp. We did not test EBA against hERG 1b alone because (i) the difference in potency between 1a and 1a/1b was marked and native I_{Kr} channels are not comprised of hERG1b alone and (ii) recordings of hERG 1b alone were comparatively difficult to obtain (presumably due to the RXR ER retention motif on this isoform[16]) – consequently, we restricted hERG1b recordings to the drugs that showed no difference between hERG1a and hERG1a/1b. On the basis of the current findings, future structure-function work with EBA is warranted to determine its binding site(s) on the hERG channel, comparing the hERG 1a and 1b isoforms.

In terms of preclinical screening of novel drugs, it might be argued that differences in potencies between hERG1a and 1a/1b are relatively modest and are likely to fall within a range similar to interlaboratory, interprotocol, or preparation differences for hERG1a. This might suggest that experiments on hERG1a alone are sufficiently reliable for screening of novel chemical entities. For the most part such as assertion might hold; however, there are likely to be some exceptions, perhaps particularly in the case of drugs that may not interact primarily with the canonical pore-binding site. Therefore, for the most promising novel compounds, it would be prudent either to incorporate additional concentration-response measurements for hERG1a/1b for comparison with hERG 1a, or to incorporate AP measurements to place hERG1a data in the context of physiological events in native tissue. The CiPA initiative embodies such an approach through the use of hIPSC-derived myocytes, which express human I_{Kr} comprised of both hERG1a and 1b isoforms.[16]

Acknowledgments

The authors thank the British Heart Foundation (BHF) and Heart Research UK (HRUK) for support: BHF (PG/10/96/28661; FS/11/59/28938) and HRUK RG2640/14/16. JCH also acknowledges the receipt of a University of Bristol Research Fellowship.

Financial support and sponsorship

Nil.

Conflicts of interest

There are no conflicts of interest.

References

1. Carmeliet E. Potassium channels in cardiac cells. Cardiovasc Drugs Ther 1992;6:305-12.
2. Tamargo J, Caballero R, Gomez R, Valenzuela C, Delpon E. Pharmacology of cardiac potassium channels. Cardiovasc Res 2004;62:9-33.
3. Virág L, Iost N, Opincariu M, Szolnoky J, Szécsi J, Bogáts G, *et al.* The slow component of the delayed rectifier potassium current in undiseased human ventricular myocytes. Cardiovasc Res 2001;49:790-7.
4. Gima K, Rudy Y. Ionic current basis of electrocardiographic waveforms: A model study. Circ Res 2002;90:889-96.
5. Sanguinetti MC, Jiang C, Curran ME, Keating MT. A mechanistic link between an inherited and an acquired cardiac arrhythmia: HERG encodes the I_{Kr} potassium channel. Cell 1995;81:299-307.
6. Robertson GA, Jones EM, Wang J. Gating and assembly of heteromeric hERG1a/1b channels underlying I(Kr) in the heart. Novartis Found Symp 2005;266:4-15.
7. London B, Trudeau MC, Newton KP, Bayer AK, Copeland NG, Gilbert DJ, *et al*. Two isoforms of the mouse ether-à-go-go related gene coassemble form channels with properties similar to the rapidly activating component of the cardiac delayed rectifier K current. Circ Res 1997;81:870-8.
8. Jones EM, Roti Roti EC, Wang J, Robertson GA. Cardiac I_{Kr} channels minimally comprise hERG 1a and 1b subunits. J Biol Chem 2004;279:44690-4.
9. Sale H, Wang J, O'Hara TJ, Tester DJ, Phartiyal P, He JQ, *et al.* Physiological properties of hERG 1a/1b heteromeric currents and a hERG 1b-specific mutation associated with long-QT syndrome. Circ Res 2008;103:e81-95.
10. Larsen AP, Olesen SP, Grunnet M, Jespersen T. Characterization of hERG1a and hERG1b potassium channels-a possible role for hERG1b in the $I_{(Kr)}$ current. Pflugers Arch 2008;456:1137-48.
11. Larsen AP. Role of ERG1 isoforms in modulation of ERG1 channel trafficking and function. Pflugers Arch 2010;460:803-12.
12. Lees-Miller JP, Kondo C, Wang L, Duff HJ. Electrophysiological characterization of an alternatively processed ERG K^+ channel in mouse and human hearts. Circ Res 1997;81:719-26.
13. Wang J, Trudeau MC, Zappia AM, Robertson GA. Regulation of deactivation by an amino terminal domain in human ether-à-go-go-related gene potassium channels. J Gen Physiol 1998;112:637-47.
14. Wang J, Myers CD, Robertson GA. Dynamic control of deactivation gating by a soluble amino-terminal domain in HERG K^+ channels. J Gen Physiol 2000;115:749-58.
15. Phartiyal P, Jones EM, Robertson GA. Heteromeric assembly of human ether-à-go-go-related gene (hERG) 1a/1b channels occurs cotranslationally via N-terminal interactions. J Biol Chem 2007;282:9874-82.
16. Jones DK, Liu F, Vaidyanathan R, Eckhardt LL, Trudeau MC, Robertson GA, *et al.* HERG 1b is critical for human cardiac repolarization. Proc Natl Acad Sci U S A 2014;111:18073-7.
17. Jones DK, Liu F, Dombrowski N, Joshi S, Robertson GA. Dominant negative consequences of a hERG 1b-specific mutation associated with intrauterine fetal death. Prog Biophys Mol Biol 2016;120:67-76.
18. Phartiyal P, Sale H, Jones EM, Robertson GA. Endoplasmic reticulum retention and rescue by heteromeric assembly regulate human ERG 1a/1b surface channel composition. J Biol Chem 2008;283:3702-7.
19. Witchel HJ, Hancox JC. Familial and acquired long QT syndrome and the cardiac rapid delayed rectifier potassium current. Clin Exp Pharmacol Physiol 2000;27:753-66.
20. Vandenberg JI, Walker BD, Campbell TJ. HERG K^+ channels: Friend and foe. Trends Pharmacol Sci 2001;22:240-6.
21. Hancox JC, McPate MJ, El Harchi A, Zhang YH. The hERG potassium

channel and hERG screening for drug-induced torsades de pointes. Pharmacol Ther 2008;119:118-32.
22. Sanguinetti MC, Tristani-Firouzi M. HERG potassium channels and cardiac arrhythmia. Nature 2006;440:463-9.
23. Perry MD, Sanguinetti MC, Mitcheson JS. Revealing the structural basis of action of hERG potassium channel activators and blockers. J Physiol 2010;588:3157-67.
24. Mitcheson JS, Perry MD. Molecular determinants of high-affinity drug binding to HERG channels. Curr Opin Drug Discov Devel 2003;6:667-74.
25. Wang W, MacKinnon R. Cryo-EM structure of the open human ether-à-go-go-related K^+channel hERG. Cell 2017;169:422-30.
26. Abi-Gerges N, Holkham H, Jones EM, Pollard CE, Valentin JP, Robertson GA, *et al.* HERG subunit composition determines differential drug sensitivity. Br J Pharmacol 2011;164:419-32.
27. Gasparoli L, D'Amico M, Masselli M, Pillozzi S, Caves R, Khuwaileh R, *et al.* New pyrimido-indole compound CD-160130 preferentially inhibits the KV11.1B isoform and produces antileukemic effects without cardiotoxicity. Mol Pharmacol 2015;87:183-96.
28. Melgari D, Brack KE, Zhang C, Zhang Y, El Harchi A, Mitcheson JS, *et al.* HERG potassium channel blockade by the HCN channel inhibitor bradycardiac agent ivabradine. J Am Heart Assoc 2015;4. pii: e001813.
29. Rajamani S, Eckhardt LL, Valdivia CR, Klemens CA, Gillman BM, Anderson CL, *et al.* Drug-induced long QT syndrome: HERG K^+ channel block and disruption of protein trafficking by fluoxetine and norfluoxetine. Br J Pharmacol 2006;149:481-9.
30. Moss AJ, Morganroth J. Cardiac effects of ebastine and other antihistamines in humans. Drug Saf 1999;21 Suppl 1:69-80.
31. Sánchez-Chapula JA, Navarro-Polanco RA, Culberson C, Chen J, Sanguinetti MC. Molecular determinants of voltage-dependent human ether-a-go-go related gene (HERG) K^+ channel block. J Biol Chem 2002;277:23587-95.
32. Bustos MD, Gay F, Diquet B, Thomare P, Warot D. The pharmacokinetics and electrocardiographic effects of chloroquine in healthy subjects. Trop Med Parasitol 1994;45:83-6.
33. Khobragade SB, Gupta P, Gurav P, Chaudhari G, Gatne MM, Shingatgeri VM, *et al.* Assessment of proarrhythmic activity of chloroquine in *in vivo* and *ex vivo* rabbit models. J Pharmacol Pharmacother 2013;4:116-24.
34. Perrin MJ, Kuchel PW, Campbell TJ, Vandenberg JI. Drug binding to the inactivated state is necessary but not sufficient for high-affinity binding to human ether-à-go-go-related gene channels. Mol Pharmacol 2008;74:1443-52.
35. Milnes JT, Witchel HJ, Leaney JL, Leishman DJ, Hancox JC. Investigating dynamic protocol-dependence of hERG potassium channel inhibition at 37 degrees C: Cisapride versus dofetilide. J Pharmacol Toxicol Methods 2010;61:178-91.
36. Layton D, Key C, Shakir SA. Prolongation of the QT interval and cardiac arrhythmias associated with cisapride: Limitations of the pharmacoepidemiological studies conducted and proposals for the future. Pharmacoepidemiol Drug Saf 2003;12:31-40.
37. Severe cardiac arrhythmia on cisapride. Prescrire Int 2000;9:144-5.
38. McPate MJ, Duncan RS, Witchel HJ, Hancox JC. Disopyramide is an effective inhibitor of mutant HERG K^+ channels involved in variant 1 short QT syndrome. J Mol Cell Cardiol 2006;41:563-6.
39. McPate MJ, Duncan RS, Hancox JC, Witchel HJ. Pharmacology of the short QT syndrome N588K-hERG K^+ channel mutation: Differential impact on selected class I and class III antiarrhythmic drugs. Br J Pharmacol 2008;155:957-66.
40. Milnes JT, Crociani O, Arcangeli A, Hancox JC, Witchel HJ. Blockade of HERG potassium currents by fluvoxamine: Incomplete attenuation by S6 mutations at F656 or Y652. Br J Pharmacol 2003;139:887-98.
41. Ridley JM, Dooley PC, Milnes JT, Witchel HJ, Hancox JC. Lidoflazine is a high affinity blocker of the HERG K^+ channel. J Mol Cell Cardiol 2004;36:701-5.
42. McNally BA, Pendon ZD, Trudeau MC. hERG1a and hERG1b potassium channel subunits directly interact and preferentially form heteromeric channels. J Biol Chem 2017;292:21548-57.
43. Du CY, El Harchi A, McPate MJ, Orchard CH, Hancox JC. Enhanced inhibitory effect of acidosis on hERG potassium channels that incorporate the hERG1b isoform. Biochem Biophys Res Commun 2011;405:222-7.
44. Gintant GA. Preclinical torsades-de-pointes screens: Advantages and limitations of surrogate and direct approaches in evaluating proarrhythmic risk. Pharmacol Ther 2008;119:199-209.
45. Anon. ICH S7B Note for Guidance on the Nonclinical Evaluation of the Potential for Delayed Ventricular Repolarization (QT interval prolongation) by Human Pharmaceuticals. Reference CHMP/ICH/423/02. London; 2005.
46. Yap YG, Camm AJ. Drug induced QT prolongation and torsades de pointes. Heart 2003;89:1363-72.
47. Viskin S, Justo D, Halkin A, Zeltser D. Long QT syndrome caused by noncardiac drugs. Prog Cardiovasc Dis 2003;45:415-27.
48. Zeltser D, Justo D, Halkin A, Prokhorov V, Heller K, Viskin S, *et al.* Torsade de pointes due to noncardiac drugs: Most patients have easily identifiable risk factors. Medicine (Baltimore) 2003;82:282-90.
49. Redfern WS, Carlsson L, Davis AS, Lynch WG, MacKenzie I, Palethorpe S, *et al.* Relationships between preclinical cardiac electrophysiology, clinical QT interval prolongation and torsade de pointes for a broad range of drugs: Evidence for a provisional safety margin in drug development. Cardiovasc Res 2003;58:32-45.
50. Witchel HJ, Milnes JT, Mitcheson JS, Hancox JC. Troubleshooting problems with *in vitro* screening of drugs for QT interval prolongation using HERG K^+ channels expressed in mammalian cell lines and xenopus oocytes. J Pharmacol Toxicol Methods 2002;48:65-80.
51. Kirsch GE, Trepakova ES, Brimecombe JC, Sidach SS, Erickson HD, Kochan MC, *et al.* Variability in the measurement of hERG potassium channel inhibition: Effects of temperature and stimulus pattern. J Pharmacol Toxicol Methods 2004;50:93-101.
52. Yao JA, Du X, Lu D, Baker RL, Daharsh E, Atterson P, *et al.* Estimation of potency of HERG channel blockers: Impact of voltage protocol and temperature. J Pharmacol Toxicol Methods 2005;52:146-53.
53. Polak S, Wiśniowska B, Brandys J. Collation, assessment and analysis of literature *in vitro* data on hERG receptor blocking potency for subsequent modeling of drugs' cardiotoxic properties. J Appl Toxicol 2009;29:183-206.
54. Wiśniowska B, Polak S. HERG *in vitro* interchange factors – Development and verification. Toxicol Mech Methods 2009;19:278-84.
55. Takasuna K, Katsuyoshi C, Manabe S. Pre-clinical QT risk assessment in pharmaceutical companies- issues of current QT risk assessment. Biomolecules Ther 2009;17:1-11.
56. Sager PT, Gintant G, Turner JR, Pettit S, Stockbridge N. Rechanneling the cardiac proarrhythmia safety paradigm: A meeting report from the cardiac safety research consortium. Am Heart J 2014;167:292-300.
57. Fermini B, Hancox JC, Abi-Gerges N, Bridgland-Taylor M, Chaudhary KW, Colatsky T, *et al.* A new perspective in the field of cardiac safety testing through the comprehensive *in vitro* proarrhythmia assay paradigm. J Biomol Screen 2016;21:1-11.
58. Weerapura M, Nattel S, Chartier D, Caballero R, Hebert TF. A comparison of currents carried by HERG with and without the coexpression of MiRP1, and the native rapid delayed rectifier current. Is MiRP1 the missing link? J Physiol 2002;540:15-27.
59. Noveck RJ, Preston RA, Swan SK. Pharmacokinetics and safety of ebastine in healthy subjects and patients with renal impairment. Clin Pharmacokinet 2007;46:525-34.
60. Ko CM, Ducic I, Fan J, Shuba YM, Morad M. Suppression of mammalian K^+ channel family by ebastine. J Pharmacol Exp Ther 1997;281:233-44.
61. Mitcheson JS, Chen J, Lin M, Culberson C, Sanguinetti MC. A structural basis for drug-induced long QT syndrome. Proc Natl Acad Sci U S A 2000;97:12329-33.
62. Kamiya K, Niwa R, Mitcheson JS, Sanguinetti MC. Molecular determinants of HERG channel block. Mol Pharmacol 2006;69:1709-16.
63. Imai YN, Ryu S, Oiki S. Docking model of drug binding to the human ether-à-go-go potassium channel guided by tandem dimer mutant patch-clamp data: A synergic approach. J Med Chem 2009;52:1630-8.